論文 / 著書情報
Article / Book Information

Title	Perpendicular-Corporate Feed in Three-Layered Parallel-Plate Radiating-Slot Array
Authors	Hisanori Irie, Jiro Hirokawa
Citation	IEEE TRANSACTIONS ON ANTENNAS AND PROPAGATION, Vol. 65, No. 11, pp. 5829-5836
Pub. date	2017, 11
Copyright	(c) 2017 IEEE. Personal use of this material is permitted. Permission from IEEE must be obtained for all other uses, in any current or future media, including reprinting/republishing this material for advertising or promotional purposes, creating new collective works, for resale or redistribution to servers or lists, or reuse of any copyrighted component of this work in other works.
DOI	http://dx.doi.org/10.1109/TAP.2017.2751659
Note	This file is author (final) version.

1) What is the problem being addressed by the manuscript and why is it important to the Antennas & Propagation community? (limited to 100 words):

The paper addresses the structural problem on the need of the metal contact by the diffusion bonding of laminating metal plates in the double-layer corporate-feed slot array antennas. To remove the metal contact in the radiating part, we introduce dielectric with proper permittivity in some part of the radiating part. The dielectric excites a standing wave in the region and provides uniform excitation for the array. This technology supports to advance the performance of planar array antennas for the millimeter-wave applications in terms of fabrication.

2) What is the novelty of your work over the existing work? (limited to 100 words)

The paper presents a novel feeding structure defined as a perpendicular-corporate feed for a three-layered parallel-plate slot array and its design process. The feeding structure contributes to removing the x-shaped cavity walls completely in the radiating part of the conventional planar corporate-feed waveguide slot array antenna. We place dielectric with proper permittivity in the region between the coupling-aperture and the radiating-slot layer to excite a standing wave strongly there for a large number of slots. The proposed structure features the uniform excitation for its 16×16-element array owning to the standing wave.

3) Provide up to three references, published or under review, (journal papers, conference papers, technical reports, etc.) done by the authors/coauthors that are closest to the present work. Upload them as supporting documents if they are under review or not available in the public domain. Enter "N.A." if it is not applicable.

* H. Irie, and J. Hirokawa, "Feasibility of perpendicular-corporate feed for a multi-layered parallel-plate slot array antenna," Proc. Euro. Conf. Antenna Propag., pp. 3109-3110, Mar. 2017.
* Y. Miura, J. Hirokawa, M. Ando, Y. Shibuya, and G. Yoshida, "Double-layer full-corporate-feed hollow-waveguide slot array antenna in the 60-GHz band," IEEE Trans. Antennas Propag., vol.59, no.8, pp.2844-2851, Aug. 2011.

4) Provide up to three references (journal papers, conference papers, technical reports, etc.) done by other authors that are most important to the present work. Enter "N.A." if it is not applicable.

N.A.

Perpendicular-Corporate Feed in Three-Layered Parallel-Plate Radiating-Slot Array

Hisanori Irie, and Jiro Hirokawa, *Fellow, IEEE*

***Abstract*— We propose a perpendicular-corporate feed in a three-layered parallel-plate radiating-slot array to remove the x-shaped cavity walls completely in the radiating part of the conventional planar corporate-feed waveguide slot array antenna. Coupling apertures on the bottom excite radiating slots spaced with the half of their spacing on the middle in the parallel plates. We place dielectric with proper permittivity in the region between the coupling-aperture and the radiating-slot layer to excite a standing wave strongly there for a large number of slots. A parasitic-slot layer is added on the top to improve the bandwidth. A 16×16-slot array antenna is designed for uniform excitation with the perpendicular and the planar corporate-feeds, and fabricated in the 60 GHz band. At the design frequency of 61.5 GHz, the measured directivity is 33.5 dBi with the aperture efficiency of 90.6 %.**

***Index Terms*— parallel plates, slot array, perpendicular-corporate feed.**

I. Introduction

Planar array antennas are suitable for millimeter-wave applications such as automotive radars and wireless communications [1] - [3]. The millimeter-wave applications require high gain antennas because such a higher frequency band has much more atmospheric attenuation caused by oxygen and vapor than a lower frequency band [4], [5]. In addition, a wideband characteristic of about 15 - 20 % fractal bandwidth is required for these applications.

We have proposed the corporate-feed waveguide slot array antennas, which are fabricated by the diffusion bonding of the laminated thin copper plates [6] - [8]. The diffusion bonding is a commercially available fabrication technique, whose advantageous features are high accuracy, reproducibility, reliability, and suitability for mass-production. The antenna consists of a radiating-slot layer, a cavity layer, a coupling-aperture layer, and a planar corporate-feed circuit layer. The planar corporate-feed circuit is a tournament-type feeding structure composed of H-plane T-junctions. It feeds the coupling apertures. Then, each coupling aperture excites 2×2 radiating slots through in the cavity. The cavity can hold electromagnetic field without leakage by its x-shaped walls. We have achieved the high antenna efficiency by using hollow waveguides, and the wide bandwidth by using the corporate feed.

Recently, the corporate-feed waveguide slot array antennas based on [6] have been advanced by using various technologies. Some of them are as follows. cavity-backed patch antenna arrays with a full corporate substrate integrated waveguide feed networks were reported [9]. The antenna composed of 16×16 radiating elements is fabricated by applying the standard printed circuit board (PCB) technology. The measured results provided gain up to 30.1 dBi with a 3-dB gain bandwidth of 16.1 % and the bandwidth of 15.3 % for VSWR < 2. The direct metal laser sintering 3-D printing technique was used to fabricate an 8×8 waveguide array with an integrated corporate-fed network [10]. The measured results showed greater than 80 % antenna efficiency and the bandwidth of 12.6 % (14.17 - 16.07 GHz) for VSWR < 2. Above-mentioned antennas are fabricated with metal contact of each layer. To remove the metal contact in the feeding circuit, a 76 GHz multi-layered phased array antenna using waffle-iron ridge waveguides was proposed [11], [12]. The structure has waffle-iron conductor rods, which are a quarter wavelength in height and allows the top surface of rods to form EMB (Equivalent Magnetic Boundary). The EMB enables the electromagnetic to propagate between two parallel plates without the metal contact. The structure has an advantage of avoiding losses due to imperfect metal contacts. In addition, a corrugated slot antenna array with ridge gap waveguide was studied [13] – [15]. There is also no requirement of metal contact between three layers owning to the parallel plates with the EMB in the feed circuit. The measured results demonstrated larger than 32.5 dBi over the 60 GHz band with more than 70 % antenna efficiency and the bandwidth of 15.3% for VSWR < 2 [15].

In this paper, we propose a perpendicular-corporate feed in a three-layered parallel-plate radiating slot array as shown in Fig. 1. It is to remove the x-shaped cavity walls completely in the radiating part of the conventional planar corporate-feed waveguide slot array antenna [6]. Coupling apertures on the bottom excite radiating slots spaced with the half of their spacing on the middle in the parallel plates. In other words, the spacing of the radiating slots is twice that of the coupling apertures. This means the corporate feed is achieved in the perpendicular direction so that the number ratio of the radiating slots over the coupling apertures is 4:1 in a two-dimensional array. Dielectric with proper permittivity is placed in the region between the coupling-aperture layer and the radiating-slot layer so that the equivalent spacing of the coupling apertures and the radiating slots are two and one wavelength in this dielectric-filled region, respectively, to excite a standing wave strongly there for a large number of slots [16], [17]. When the radiating-slot layer is only introduced, the bandwidth is narrow. A parasitic-slot layer is added over the radiating-slot layer to enhance the bandwidth.

We presented only the effect of dielectric in the parallel plates as feasibility study in [18] and did not include the planar corporate-feed circuit. This paper reveals a full model analysis which includes the planar corporate-feed circuit and experimental results. The paper is organized as follows. Section II describes the antenna configuration. In section III, we present

The authors are with the Department of Electrical and Electric Engineering, Tokyo Institute of Technology, Tokyo, 152-8552, Japan (e-mail: irie.h@antenna.ee.titech.ac.jp; jiro@antenna.ee.titech.ac.jp).

the design procedure of the perpendicular-corporate feed by using a 2×2-element subarray. An 8×8-element subarray is analyzed to demonstrate the effect of the dielectric. The effect of parasitic slots for wideband design is confirmed. The simulated results of a 16×16-element array fed by a planar corporate-feed circuit are provided. In section IV, we compare the measured results of the fabricated antenna with the simulated ones.

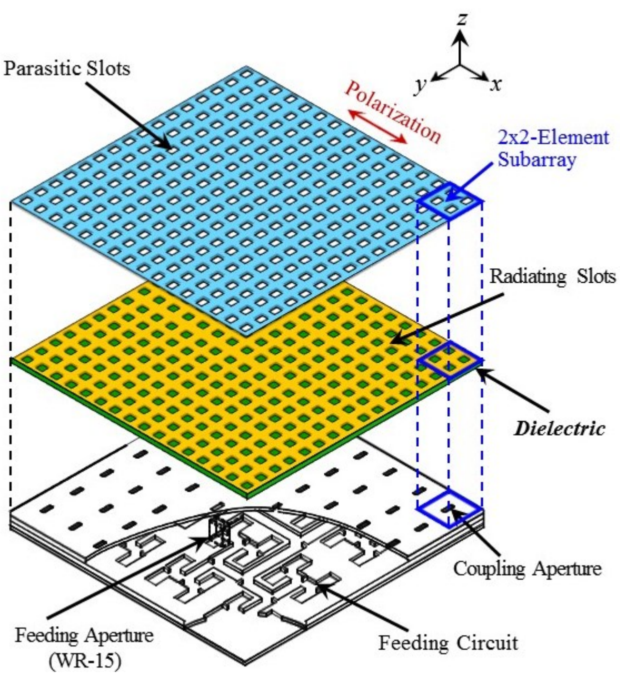

Fig1. Three-Layered Parallel-Plate 16×16 Radiating Slot Array Fed by a Perpendicular-Corporate Feed

II. ANTENNA CONFIGURATION

Fig. 1 shows the three-layered parallel-plate 16×16 radiating slot array fed by a perpendicular-corporate feed. The antenna consists of layers of parasitic slots, radiating slots, dielectric, coupling apertures, and a planar feeding circuit. In Fig.1, the layers are described with a distance to show the internal structure. However, in the actual antenna, they are stacked. The antenna is fed by a feed aperture, which is the same size as the standard waveguide WR-15, from its backside. The feeding circuit is a planar corporate feed composed of H-plane T-junctions. The coupling apertures are placed between the feeding circuit and the dielectric. The radiating slots are mounted on the dielectric. The parasitic slots are placed on the top of the radiating slots with a spacing. The spacing between the radiating and the parasitic slots is hollow. For radiating slots and parasitic ones, the slot spacing is constant: $0.86\lambda_0$ (4.20 mm) in the x and y directions. λ_0 is the wavelength at the design frequency of 61.5 GHz. The polarization is along the x-axis.

III. DESIGN

A. Effect of Dielectric

Fig. 2 shows the structural difference between the proposed and the conventional models for the 2×2-element subarray. In the external regions, two sets of periodic boundaries and radiation boundary are introduced as well as in Fig.5, even though they are not shown in Fig.2. The two sets of periodic boundaries are used to include the mutual coupling in the infinite two-dimensional array. The conventional model holds field in the x-shaped cavity by the side walls of PEC (perfect electrical conductor). On the other hand, the proposed model removes the side walls and fills dielectric with proper permittivity in the region between the coupling-aperture layer and the radiating-slot layer so that the effective electrical size increases from 1.72 free-space wavelength to two wavelengths (about $1.72\lambda_0 \times \sqrt{\varepsilon_r}$). They lead to exciting a standing wave in the region. The pink parallelograms are ports for the simulations.

We design a 16×16-element array. Fig. 3 is the analysis model of the 8×8-element subarray including the symmetry of the 16×16-element array. The radiating-slot layer with dielectric, and PEC, PMC (perfect magnetic conductor) and radiation boundaries at the front are described with a distance from the coupling-aperture layer to show the internal structure of the feed. Each of the coupling apertures is fed by a longitudinal coupling aperture on the broad wall of a waveguide as shown in Fig. 2 (b). Around the periphery of the 8×8-element subarray, PEC boundaries parallel to the yz-plane and PMC boundaries parallel to the xz-plane are introduced for the x-polarized operation. The parallel plates are truncated by PEC and PMC by considering the polarization. For the external region, radiation boundaries are introduced for analyzing by ANSYS HFSS Ver. 16.

† The distance between elements is constant: $0.86\lambda_0$

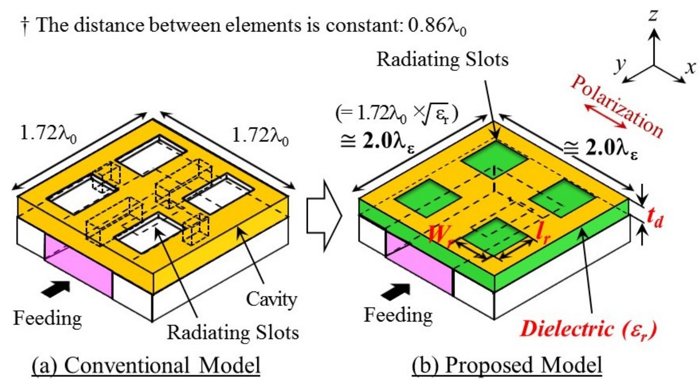

Fig. 2. Difference Between the Proposed and the Conventional Models

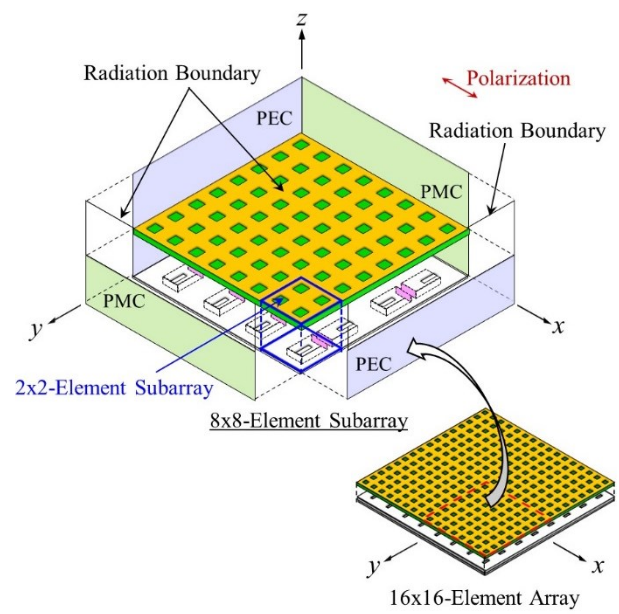

Fig. 3. Analysis Model of 8×8-Element Subarray

We analyze both the 2×2-element and the 8×8-element subarrays. The parameters are the size l_r and w_r of the radiating slots, the thickness t_d of the dielectric and its relative permittivity ε_r as shown in Fig. 2 (b). These parameters are determined so that the desired operation can be achieved where the frequency characteristic of the reflection of the 16 coupling apertures should be identical in the 8×8-element subarray and it should agree with that of the 2×2-element subarray. Furthermore, the other parameters relating to the coupling aperture are determined to minimize the reflection at the design frequency. Once the desired operation is achieved, all the radiating slots are excited uniformly because of their periodic arrangement.

Fig. 4 shows the frequency characteristics of reflections from 16 coupling apertures in the 8×8 radiating slot subarray by 16 gray lines for $\varepsilon_r = 1.00$ and $\varepsilon_r = 1.28$. A red dashed line shows the reflection from the coupling aperture in the 2×2 radiating slot subarray as reference. For $\varepsilon_r = 1.28$ the above-mentioned desired operation is achieved while for $\varepsilon_r = 1.00$ it is not. When the dielectric constant is changed, the effective wavelength in the dielectric region is changed. As a result, for $\varepsilon_r = 1.28$, the effect from a radiating slot to adjacent slots and that from the adjacent slots to the radiating slot are balanced, so that all the radiating slots in the 8×8-element subarray are expected to excite uniformly. However, for $\varepsilon_r = 1.00$, these two effects are unbalanced, so that the radiating slots in the 8×8-element subarray are excited differently. The effect of the dielectric is confirmed. However, the bandwidth for the reflection less than -14 dB is very narrow, which is about 0.5 %.

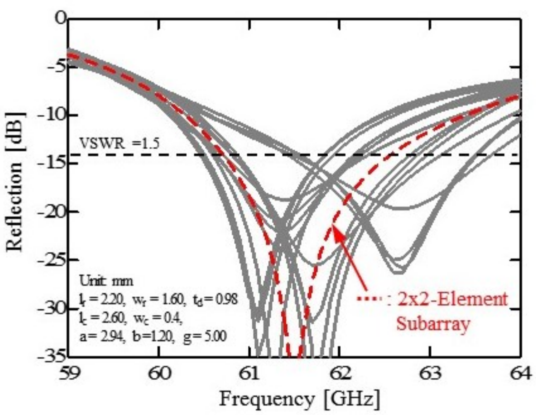

(a) $\varepsilon_r = 1.00$

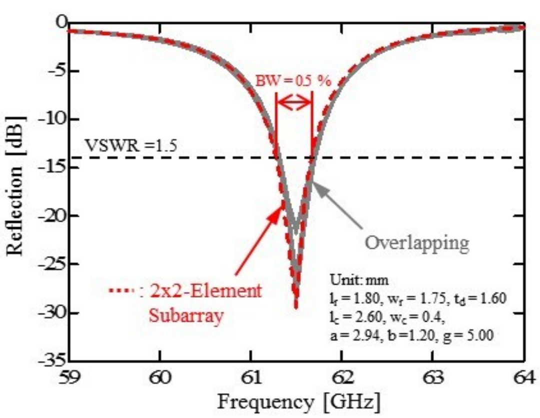

(b) $\varepsilon_r = 1.28$

Fig. 4. Frequency Characteristic of Reflection

B. Parasitic Slots

To improve the bandwidth for $\varepsilon_r = 1.28$, we place the parasitic-slot layer over the radiating-slot layer with a spacing. Fig. 5 shows a 2×2-element subarray with parasitic slots. The parameters are the size of the parasitic slots: l_p and w_p, and the spacing between the parasitic-slot and the radiating-slot layers: h_{pr}. We also include l_r, w_r and t_d into the parameters in the analysis. Fig. 6 shows the analysis model of the 8×8-element subarray with the parasitic-slot layer. The design procedure is the same to that of the previous subsection.

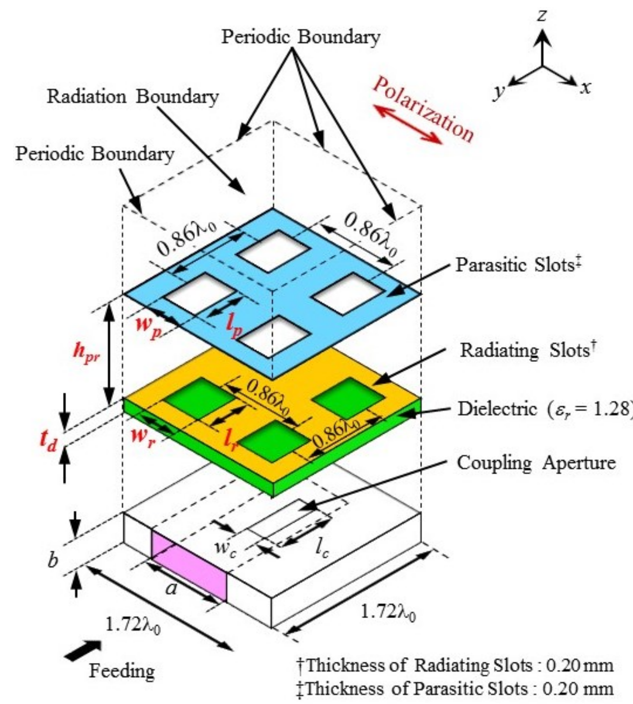

Fig. 5. 2×2-Element Subarray with Parasitic Slots

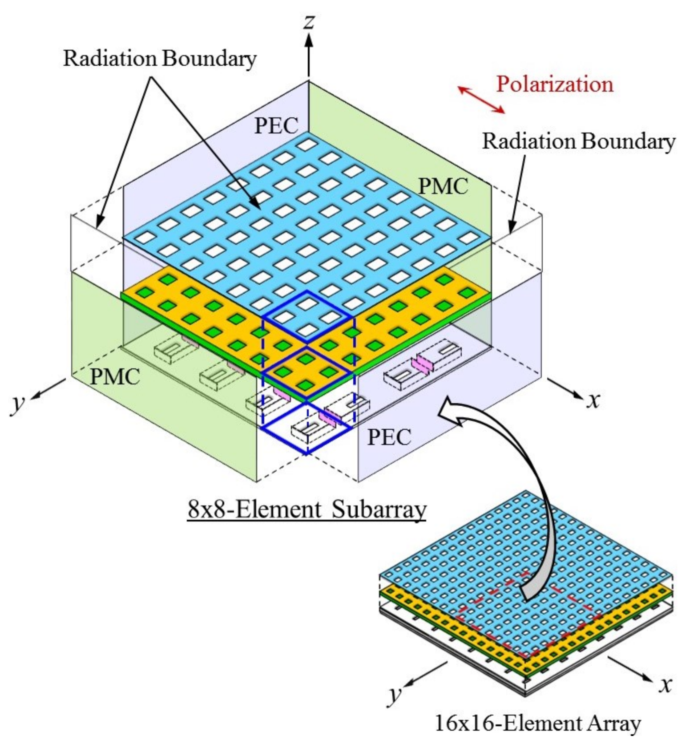

Fig. 6. 8×8-Element Subarray with Parasitic Slots

Fig. 7 shows the frequency characteristic of the reflection. The reflection of the 2×2-element subarray is less than -14 dB over 7.7 % bandwidth ranging from 59.1 GHz to 63.9 GHz. The bandwidth is improved from 0.5 % to 7.7 % by placing the parasitic-slot layer. The deviation of the frequency characteristics of the reflection among the 16 coupling apertures in the 8×8-element subarray cannot be suppressed completely; however, it is small.

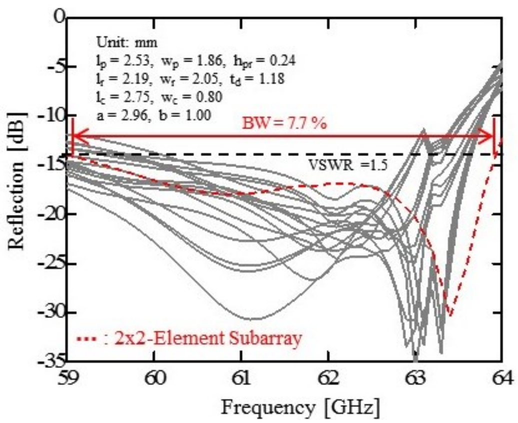

Fig. 7. Frequency Characteristic of Reflection

C. Simulated Result of 16×16-Element Array Antenna

Fig. 8 shows the full structure of the three-layered parallel-plate 16×16-slot array antenna fed by the planar corporate-feed circuit. In Fig.8, the plates are described with a distance to show the internal structure. However, in the actual antenna, they are stacked. In the simulation, the conductivity 5.8×10^7 S/m of copper and the loss tangent 0.002 of the dielectric are assumed. The periphery of the three-layered parallel plates is terminated by copper by considering the fabrication to keep the flatness. Note that this copper termination does not mean to make a large cavity for the antenna operation. The operation as the large cavity could degrade the antenna characteristics. All the metal plates are connected by fixing screws in the fabrication.

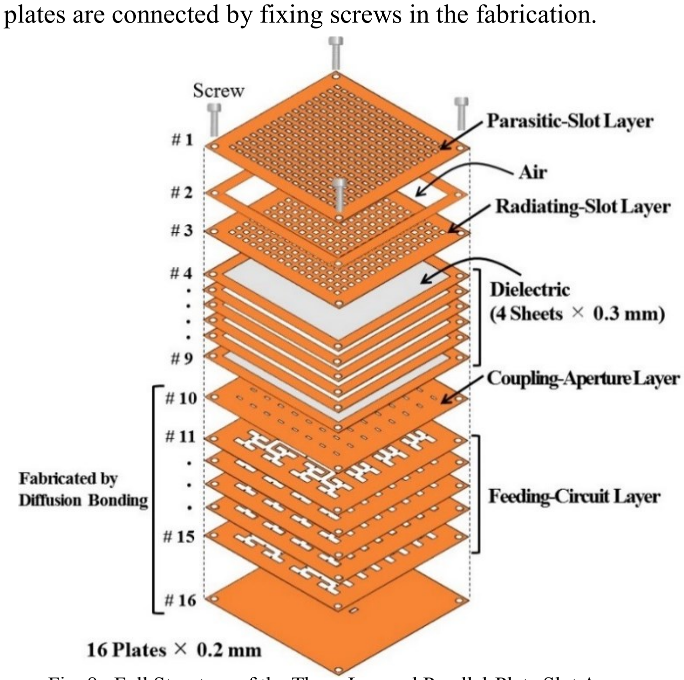

Fig. 8. Full Structure of the Three-Layered Parallel-Plate Slot Array Fed by Planar Corporate Feed

The edge as PMC of the parallel plates only in the *y* direction is extended by 1.2 mm (≈ $0.25\lambda_0$) and terminated by a conductor. The dimension of the antenna in the *xy*-plane is 81.0 mm × 79.0 mm. Although we slightly modify only h_{pr} (0.24 → 0.20 mm) and t_d (1.18 → 1.20 mm) to consider the fabrication limitation on the thickness of the copper plate and the dielectric, the parameters of the antenna are the same as the 8×8-element array with the parasitic-slot layer

Fig. 9 shows the frequency characteristic of the reflection. The reflection of the antenna is less than -14 dB over 7.3 % bandwidth ranging from 59.1 GHz to 63.6 GHz. The bandwidth is the almost same as that of the 2×2-element subarray. The reflection of the antenna has a ripple caused by the reflection of the planar corporate-feed circuit. The final design parameters are listed in Table I.

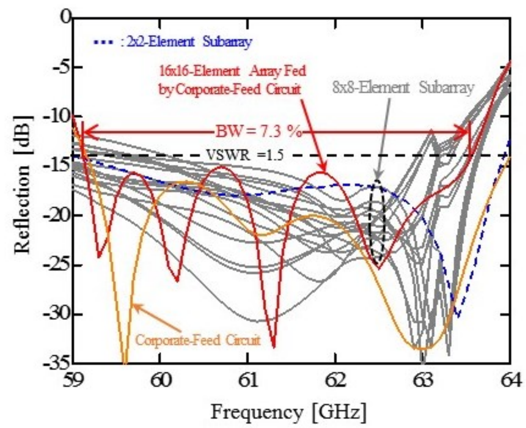

Fig. 9. Frequency Characteristic of Reflection

TABLE I
DESIGN PARAMETERS OF THREE-LAYERED PARALLEL-PLATE 16×16-SLOT ARRAY ANTENNA FED BY PLANAR CORPORATE FEED

Fixed Parameters		
Relative permitivity of the Dielectric	ε_r	1.28
Dielectric loss tangent	$tan\,\delta$	0.002
Width of the Feeding Waveguide	a	2.96 mm
Thickness of the Feeding Waveguide	b	1.00 mm
Length of the Coupling Aperture	l_c	2.75 mm
Width of the Coupling Aperture	w_c	0.80 mm
Thickness of the Bottom of the Feeding WG	-	0.20 mm
Thickness of the Coupling Aperture	-	0.20 mm
Thickness of Radiating Slot	-	0.20 mm
Thickness of the Parasitic Slot	-	0.20 mm
Variable Parameters		
Length of Radiating Slot	l_r	2.19 mm
Width of Radiating Slot	w_r	2.05 mm
Thickness of the Dielectric	t_d	1.20 mm
Length of the Parasitic Slot	l_p	2.53 mm
Width of the Parasitic Slot	w_p	1.86 mm
Spacing Between the Par. Slot and Rad. One	h_{pr}	0.20 mm

IV. EXPERIMENTAL RESULT

Fig. 10 shows the picture of the fabricated antenna. The total number of plates is 16. The feeding-circuit layer with the coupling-aperture layer composed of 7 plates is fabricated by the diffusion bonding of laminated thin copper plates. We screw the rest of plates with the feeding-circuit layer including the coupling-aperture layer after putting the dielectric between the coupling-aperture layer and the radiating-slot layer. The material of the dielectric is porous PTFE (Polytetrafluoroethylene). Its relative permittivity is 1.25 in the measurements, which is slightly smaller than that in the simulations. The region between the radiating and parasitic-slot layers is mechanically supported by a copper frame (plate #2) as shown in Fig. 8. The dimension of each plate is 79.0 mm × 81.0 mm. The total thickness of the fabricated antenna is 3.2 mm; 1.2 mm for the feeding-circuit layer, 0.2 mm for the coupling-aperture layer, 1.2 mm for the dielectric, 0.2 mm for the radiating-slot layer, 0.2 mm for the spacing between the radiating-slot and the parasitic-slot layers, and 0.2 mm for the parasitic-slot layer. We attach a choke flange, whose thickness is 6.0 mm, to the antenna by screws to connect a standard WR-15 waveguide for the measurement. The thickness of 6.0 mm is not required for the antenna operation, but for inserting the choke flange pins.

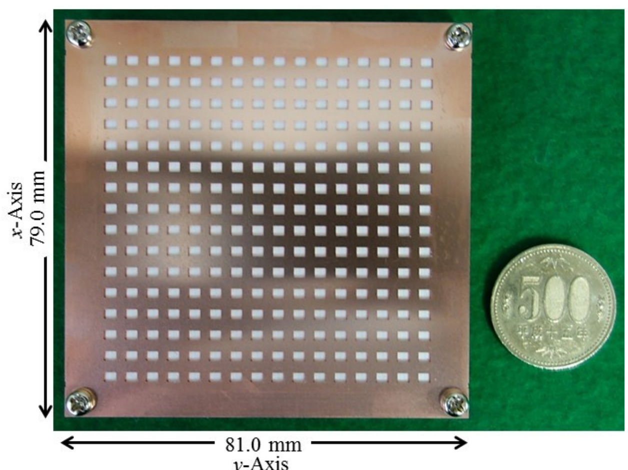

(a) Top View

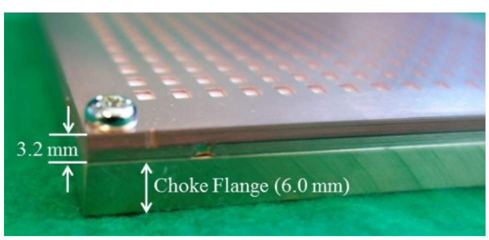

(b) Side View

Fig. 10. Picture of the Fabricated Antenna

Fig. 11 shows the measured and the simulated reflection characteristics. Each result includes the reflection characteristics of a choke flange. There is a large reflection in measurement. To identify the reason, Fig. 12 shows the time-gating analysis by a vector network analyzer (VNA). The frequency range used in the VNA is from 56 GHz – 94 GHz. The time domain response has two large reflections as shown in Fig. 12 (a). We estimate one comes around the feeding aperture and the other comes around the radiating part. The frequency domain response from each of them is added in Fig. 12 (b). The reflection around the radiating part is comparable with the overall reflection from 58 GHz to 65 GHz. However, the reflection around the feeding aperture is small around this frequency band. We conclude the main reason of the large reflection comes around the radiating part. In order to support this reason, we simulate reflection by changing the relative permittivity of the dielectric as shown in Fig. 13. Lower permittivity can simulate the large reflection in measurement. The region between the radiating-slot layer and coupling-aperture layer is filled by stacking four thin dielectric sheets. Small air gaps among the dielectric sheets could be created, which decrease the relative permittivity equivalently. Other reasons such as the size errors in the radiating slots and parasitic slots would be possible. As an example, Fig. 14 shows the reflection for changing length of the radiating slots. The reflection is not degraded significantly for ± 20 μm change.

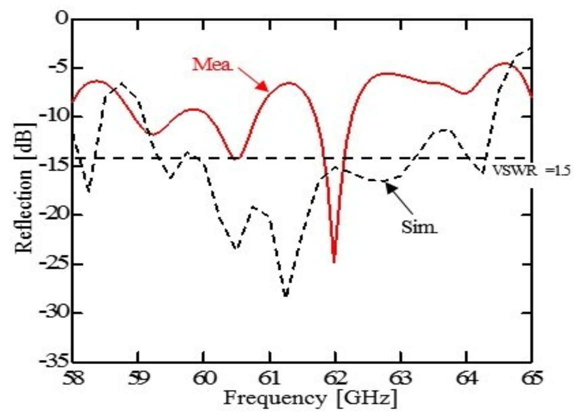

Fig. 11. Measured and Simulated Reflection Characteristics

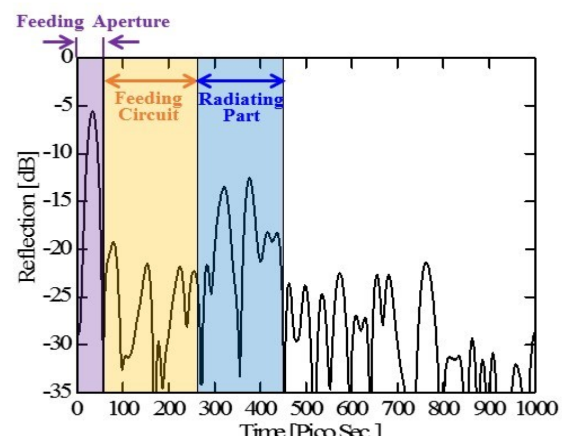

(a) Time Domain

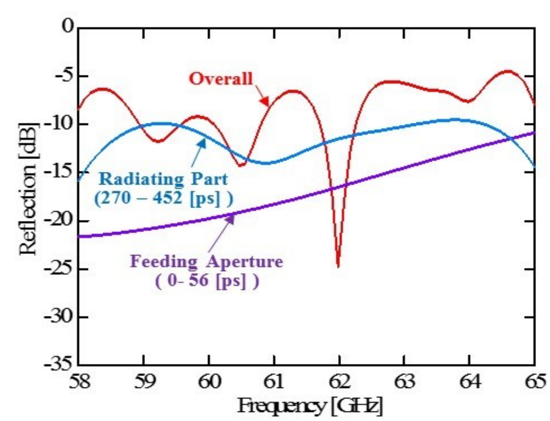

(b) Frequency Domain

Fig. 12. Time-gating Analysis

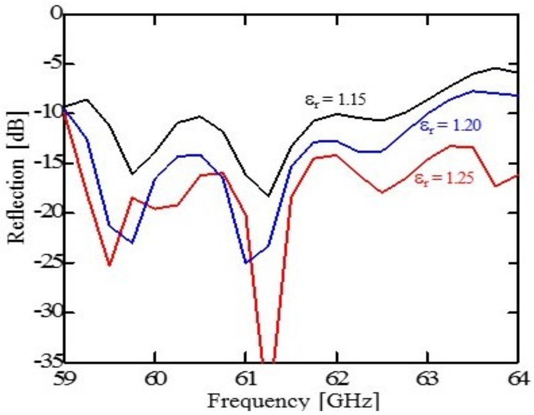

Fig. 13. Simulated Reflection Characteristics for Various Relative Permittivity of the Dielectric

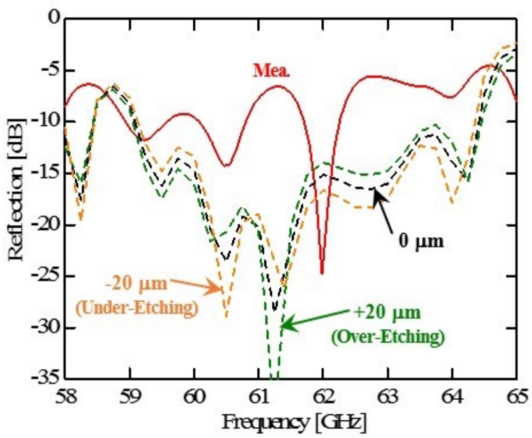

Fig. 14. Reflection for Changing Length of the Radiating Slots

Fig. 15 demonstrates the measured and the simulated amplitude, and measured phase distributions of the near-field at the design frequency of 61.5 GHz. As for the amplitude, we observe a symmetric distribution with respect to both the *x*-axis and *y*-axis. The variation in the measured amplitude is in good agreement with that of the simulated result. The measured amplitude variation over the aperture area is about 5 dB. The phase variation over the aperture area is about 60 degrees. Nevertheless, the proposed structure has a sufficient uniformity based on the configuration of radiation patterns (Fig. 16) and the efficiency of the directivity (Fig. 17).

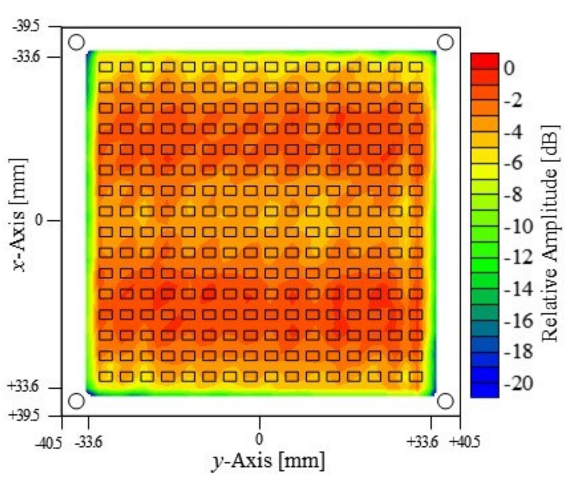

(a) Measured Amplitude

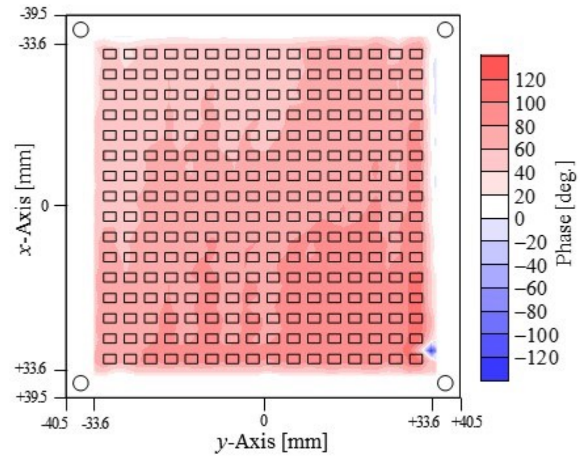

(b) Measured Phase

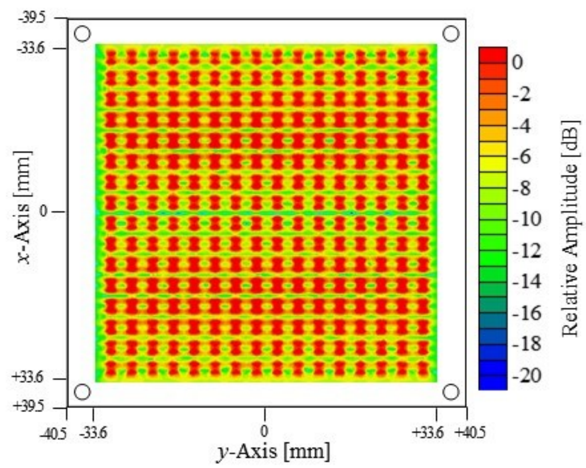

(c) Simulated Amplitude

Fig. 15. Near-Field Distribution at 61.5 GHz

Fig. 16 shows the measured and the simulated radiation patterns at 61.5 GHz in the E-plane (*xz*), H-plane (*yz*) and 45 deg.-plane. In the E-plane and H-plane, the measured patterns are in good agreement with the simulated ones. In the 45 deg.-plane, the measured pattern is almost the same as the simulated one except for ± 50-60 deg. region. The reasons of the discrepancy around ± 50-60 deg. region are not clear at this moment. The sidelobe level is small (-30 dB in simulation and -40 dB in measurement), which could not cause a problem. These patterns present uniform-excitation patterns including an element pattern. The measured first-sidelobe levels are as follows: -12.3dB at -6.5 deg., -13.2dB at +3.5 deg. in the E-plane, -12.5 dB at -6.0 deg., -13.6 dB at +6.0 deg. in the H-plane, and -26.1 dB at -9.0 deg., -25.8 dB at +9.0 deg. in the 45 deg.-plane. The structure is symmetrical in the *y*-direction, however, it is not in the *x*-direction because all the coupling slots have an offset in the same + *x*-direction. This gives slightly unsymmetrical patterns in the *xz*-plane even in the simulation. The measured pattern in each plane is not completely symmetrical because of a manufacturing error in etching and laminating processes; however, the difference is very small.

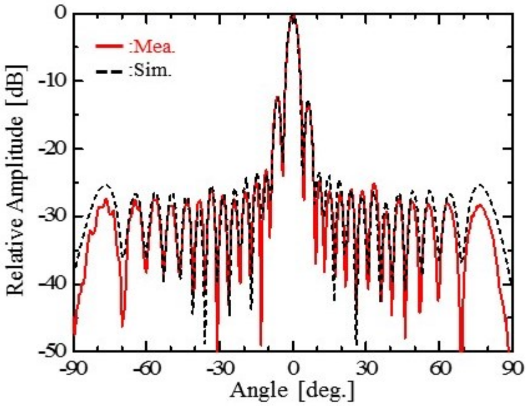

(a) E-plane (*xz*)

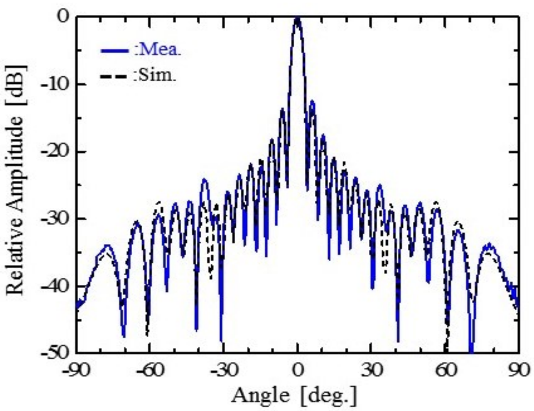

(b) H-plane (*yz*)

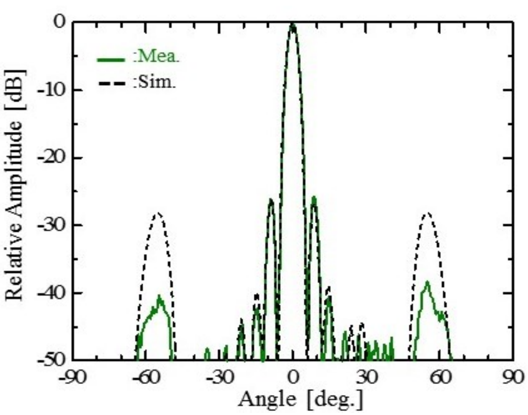

(c) 45 deg.- plane

Fig. 16. Radiation Patterns at 61.5 GHz

Fig. 17 reveals the measured and the simulated realized-gain, gain, and directivity. The realized-gain, which includes the reflection loss, and conductor and dielectric losses, is measured by the comparison with a standard gain horn antenna in an anechoic chamber. The directivity is derived from the measured near-field distribution by the Fourier transform. The measured gain is calculated by adding the measured reflection loss into the measured realized-gain. The measured realized-gain degrades comparing to the simulated one because of the reflection loss. Then, the measured gain is also degraded due to the same reason. However, the measured directivity is in good agreement with the simulated one. The aperture efficiency greater than 90 % is achieved over 5-GHz bandwidth. At the design frequency, the measured directivity is 33.5 dBi with the aperture efficiency of 90.6 % and the realized gain is 31.7 dBi with the antenna efficiency of 61.0 %.

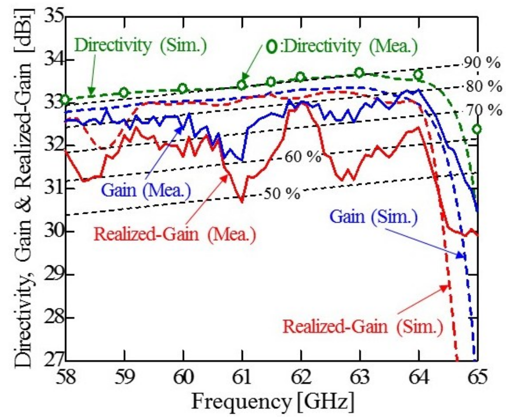

Fig. 17. Frequency Characteristics of Realized-Gain, Gain, and Directivity

V. Conclusion

In this paper, we have proposed the perpendicular-corporate feed for a three-layered parallel-plate slot array antenna. The introduction of dielectric with proper permittivity in the region between the coupling-aperture layer and the radiating-slot layer can excite uniformly by generating a standing wave. The measured amplitude distribution of the near-field demonstrates a symmetric distribution on both the *x*-axis and *y*-axis, which indicates the uniform excitation, in the 16×16-slot array antenna. The aperture efficiency greater than 90 % is achieved over 5-GHz bandwidth in the measured directivity. At the design frequency, the measured directivity is 33.5 dBi with the antenna efficiency of 90.6 %.

Acknowledgement

The authors are thankful to Mr. Naoki Shibata and Mr. Masayoshi Nakamura of Nitto Denko Corp. for providing the dielectric sheets.

References

[1] W. Menzel, D. Pilz, and R. Leberer, “A 77-GHz FM/CW radar front-end with a low-profile low-loss printed antenna,” IEEE Trans. Microw. Theory Tech., vol. 47, no. 12, pp. 2237-2241, Dec. 1999.

[2] W. Menzel, and A. Moebius, “Antenna concepts for millimeter-wave automotive radar sensors,” Proc. IEEE, vol. 100, no. 7, pp. 2372-2379, July 2012.

[3] B. Biglarbegian, M. Fakharzadeh, D. Busuioc, Mohammad-Reza Nezhad-Ahmadi, and S. Safavi-Naeini, “Optimized microstrip antenna arrays for emerging millimeter-wave wireless applications,” IEEE Trans. Antennas Propag., vol.59, no.5, pp. 1742-1747, May. 2011.

[4] R. Fellers, “Millimeter waves and their applications,” Electrical Engineering, vol. 75, no. 10, pp. 914-917, Oct. 1956.

[5] C. Tolbert, and A. Straiton, “Experimental measurement of the absorption of millimeter radio waves over extended ranges,” IEEE Trans. Antennas Propag., vol. 5, no. 2, pp. 239-241, Apr. 1957.

[6] Y. Miura, J. Hirokawa, M. Ando, Y. Shibuya, and G. Yoshida, “Double-layer full-corporate-feed hollow-waveguide slot array antenna in the 60-GHz band,” IEEE Trans. Antennas Propag., vol.59, no.8, pp.2844-2851, Aug. 2011.

[7] T. Tomura, J. Hirokawa, T. Hirano, and M. Ando, “A 45-degree linearly polarized hollow–waveguide 16 ×16-slot array antenna covering 71–86 GHz band,” IEEE Trans. Antennas Propag., vol. 62, no. 10, pp. 5061-5067, Oct. 2014.

[8] X. Xu, M. Zhang, J. Hirokawa, and M. Ando, “E-band plate-laminated waveguide filters and their integration into a corporate-feed slot array antenna with diffusion bonding technology,” IEEE Trans. Micro. Theory Tech., vol. 64, no. 11, pp. 3592 - 3603, Nov. 2016.

[9] Y. J. Li, and K. M. Luk, “60-GHz substrate integrated waveguide fed cavity-backed aperture-coupled microstrip patch antenna arrays,” IEEE Trans. Antennas Propag., vol. 63, no. 3, pp. 1075-1085, Mar. 2015.
[10] G.-L. Huang, S.-G. Zhou, T.-H. Chio, and T.-S. Yeo, “3-D metal-direct-printed wideband and high-efficiency waveguide-fed antenna array,” 2015 IEEE MTT-S Intl. Microw. Symp., DOI: 10.1109/MWSYM.2015.7166882, May 2015
[11] H. Kirino, and K. Ogawa, “A 76 GHz phased array antenna using a waffle-iron ridge waveguide,” Proc. Euro. Conf. Antenna Propag., C32P2-2, Apr. 2010.
[12] H. Kirino, and K. Ogawa, “A 76 GHz multi-layered phased array antenna using a non-metal contact metamaterial waveguide,” IEEE Trans. Antennas Propag., vol. 60, no. 2, pp. 840 - 853, Feb. 2012.
[13] P.-S. Kildal, E. Alfonso, A. Valero-Nogueira, and E. Rajo-Iglesias, “Local metamaterial-based waveguides in gaps between parallel metal plates,” IEEE Antennas Propag. Lett., vol. 8, no. 4, pp. 84-87, Apr. 2009.
[14] P. -S. Kildal, A. U. Zaman, E. Rajo-Iglesias, E. Alfonso, and A. Valero-Nogueira “Design and experimental verification of ridge gap waveguide in bed of nails for parallel-plate mode suppression,” IET Microw., Antenna Propag., vol. 5, no. 3, pp. 262-270, Feb. 2011.
[15] D. Zarifi; A. Farahbakhsh, A. Uz Zaman, and P.-S. Kildal “Design and fabrication of a high-gain 60-GHz corrugated slot antenna array with ridge gap waveguide distribution layer,” IEEE Trans. Antennas Propag., vol. 64, no. 7, pp. 2905 – 2913, July 2016.
[16] K. Tsukamoto, and H. Arai, “Characteristic of linearly polarized aperture array antenna,” IEICE Trans. Commun., vol. J78-B-II, no. 3, pp. 160-166, Mar. 1995.
[17] K. Tsukamoto, and H. Arai, “Input characteristic of tri-plate aperture array antenna,” IEICE Trans. Commun., vol. J79-B-II, no. 1, pp. 26-32, Jan. 1996.
[18] H. Irie, and J. Hirokawa, “Feasibility of perpendicular-corporate feed for a multi-layered parallel-plate slot array antenna,” Proc. Euro. Conf. Antenna Propag., pp. 3109-3110, Mar. 2017.

Hisanori Irie was born in Saitama, Japan, on December 20, 1978. He received the B.S. and M.S. degrees in electronics and information from Hosei University, Tokyo, Japan, in 2002 and 2004, respectively, and is currently working toward the D.E. degree in electrical and electric engineering from Tokyo Institute of Technology, Tokyo, Japan.

He has worked for Electric Systems Research Center, Acquisition, Technology and Logistics Agency, Ministry of Defense, Japan, since 2005. He is currently a senior researcher there.

His current research area is planar waveguide slot-array antennas.

Jiro Hirokawa (S'89-M'90-SM'03-F'12) received the B.S., M.S. and D.E. degrees in electrical and electronic engineering from Tokyo Institute of Technology (Tokyo Tech), Tokyo, Japan in 1988, 1990 and 1994, respectively.

He was a Research Associate from 1990 to 1996 and an Associate Professor from 1996 to 2015 at Tokyo Tech. He is currently a Professor there. He was with the antenna group of Chalmers University of Technology, Gothenburg, Sweden, as a Postdoctoral Fellow from 1994 to 1995.

His research area has been in slotted waveguide array antennas and millimeter-wave antennas. He received IEEE AP-S Tokyo Chapter Young Engineer Award in 1991, Young Engineer Award from IEICE in 1996, Tokyo Tech Award for Challenging Research in 2003, Young Scientists' Prize from the Minister of Education, Cultures, Sports, Science and Technology in Japan in 2005, Best Paper Award in 2007 and a Best Letter Award in 2009 from IEICE Communications Society, and IEICE Best Paper Award in 2016. He is a Fellow of IEICE.